



---

WORKING PAPER 339

REMOTE SENSING OF SOIL MOISTURE (1):  
THE VISIBLE AND REFLECTIVE  
INFRARED WAVELENGTHS

JOHN COYLE

---

**WORKING PAPER**  
**School of Geography**  
**University of Leeds**



Abstract

There are several existing techniques which relate remotely sensed data to earth surface features. Those techniques which make use of data gathered at the visible and reflective wavelengths are reviewed. In any interpretation of such data it is essential to account for scattering, absorption and attenuation of incident and reflected radiation by the atmosphere. The use of reflectance data in determining the moisture content of near-surface soils is discussed. However, soil moisture is only one of many factors which influence the reflectance properties of a surface and these are also discussed in detail. The large amount of data produced by remote sensing systems demands specialised management techniques. Data processing and pattern recognition systems are reviewed in this context.

June 1982

Remote Sensing of Soil Moisture (1):  
The Visible and Reflective Infrared Wavelengths

Contents

	Page
(1) General Introduction	2
(2) The Visible and Reflective Infrared Wavelengths	5
(3) Interaction Processes	6
(3.1) Atmospheric Effects	7
(3.2) The Reflectance Properties of the Earth's Surface	14
(4) Data Processing Systems in Remote Sensing	24
(5) General Discussion	28
(6) References	30
(7) Diagrams	

Remote Sensing of Soil Moisture.

(1). General Introduction

There is a growing need for frequent and accurate estimates of the moisture content of surface soils. This need may be identified at various levels ranging from local and regional scales to a national scale. It is felt most keenly by scientists working within the hydrological, agricultural and meteorological sciences. In these, estimates of soil moisture are crucial for modelling and planning of natural resources. For example, agricultural scientists might use estimates of soil moisture to predict crop growth and yields whilst hydrologists may use such estimates for managing water supply based on integrated models for watershed planning. It is not surprising, therefore, to find that the estimation of soil moisture has provided a focus for research for many scientists in recent years.

Conventional techniques of measuring the moisture content of surface soils suffer from two major limitations. The first of these relates to the physical disturbance of the soil by the measurement technique itself. For example, the gravimetric techniques express soil moisture as the volumetric water content of a sample of soil taken from a site. During the process of measurement, the water regime of the soil is disturbed. This tends to give rise to large errors in measurement and to limit the usefulness of the method, especially if one is attempting to monitor changes in soil

moisture over a long period of time. More advanced techniques based on neutron scattering, gamma ray attenuation or electric current flow within the soil, are subject to the same limitation although they generally avoid the need to take samples from the soil body (McKim et. al. 1980).

The second limitation relates to the high density of sampling points needed to obtain accurate estimates of soil moisture over large areas using conventional techniques. An adequate sampling density is rarely achieved because of the high cost of field observations. Estimates of soil moisture content over large areas are therefore limited in accuracy due to the large interpolations which have to be made between points. These may leave out many important features such as pockets of saturated soil (Elkington, 1979).

The measurement of soil moisture from space or airborne platforms offers a solution to these problems. Remote sensing techniques have a good potential for providing timely and comprehensive areal coverage with few of the problems of limited accessibility or sampling density of the more traditional methods of soil moisture measurement.

Several techniques have been devised for the purpose of extracting soil moisture information from remote sensor data. These fall into three broad categories based on the region of the electromagnetic spectrum within which they operate. These are:

- (1) The visible and reflective infrared waveband ( $0.38\mu\text{m}$ - $3.0\mu\text{m}$ ).
- (2) The thermal infrared waveband( $3.0\mu\text{m}$ - $15.0\mu\text{m}$ ).
- (3) The microwave waveband ( $0.3$  to  $300\text{ cm}^{-1}$ )

PAGE 4

This paper deals with the remote sensing of soil moisture within the visible and reflective part of the electromagnetic spectrum. A brief outline of the physical principles together with a review of the literature dealing with soil moisture estimation at these wavelengths is given. Complementary papers dealing with the remote sensing of soil moisture in the other two wavebands are also available.

(2). The Visible and Reflective Infra-red Wavelengths.

Introduction

Remote sensing in the wavelengths between 0.3μm to 1.3μm is mostly passive. That is, the energy source used is the reflected solar radiation from the earth and its atmosphere. Active systems, which have their own energy source (such as lasers or lidars) are, as yet, of limited usefulness for remote sensing purposes. These will not be discussed here and interested readers are referred to the Manual of Remote Sensing (Reeves, 1975). In this chapter, a brief review of remote sensing based on reflected solar energy alone is given, together with examples of practical applications in the evaluation of soil moisture.

(3) Interaction Processes

Solar radiation incident upon the earth's atmosphere is absorbed, scattered and generally attenuated by its path through the atmosphere to the ground surface, where it is reflected back into space to the sensor. The radiance measured by the sensor( $L_r$ ) can be theoretically resolved into three components for a specific wavelength( $\lambda$ ):

$$(1). \quad L_r(\lambda) = L_1(\lambda) + L_2(\lambda) + \tau \cdot \frac{M(\lambda)}{\pi}$$

$L_1$  is the radiance scattered back to the sensor by the atmosphere.  $L_2$  is the diffuse radiance reflected by one resolution element on the ground surface but is measured for a neighbouring element due to refraction and scattering by the atmosphere, (see fig.1).  $\tau$  is the transmissivity of the atmosphere and  $M(\lambda)$  is the surface exitance which is a function of the distribution of energy in space and the reflective properties of the surface.

If the properties of the ground surface are of primary importance then  $L_1$  and  $L_2$  are the main source of noise in the signal(together with errors introduced by the radiometer and processing techniques). Dave(1980) defined a 'contamination' index( $\eta$ ) to describe the extent of the 'noise':

$$(2) \quad \eta = \frac{L_1 + L_2}{L_1 + L_2 + L_3}$$

The characteristics of the measured radiation are thus dependent on firstly, the atmospheric conditions and secondly, the interaction between the incident radiation and the ground surface. These are described in turn.

(3.1) Atmospheric effects.

All shortwave radiation entering the earth's atmosphere is modified to a greater or lesser extent by the optical properties of the atmosphere. Some of these properties, such as turbulence, can be ignored for remote sensing purposes(Reeves, 1975). Scattering and absorption are the main processes involved in the attenuation of solar energy. Scattering results in the redistribution of radiation in space and is strongly wavelength dependent. Absorption is the transformation of radiant energy into heat through the interaction between specific wavelengths of radiation and molecules(e.g. ozone and ultraviolet wavelengths). The latter mechanism is responsible for the existence of 'atmospheric windows' which are wavelength bands(e.g. between 0.4um and 0.6um) where there is relatively little absorption of radiation. As a first approximation, the overall attenuation of solar radiation by the atmosphere is given by the product of scattering and absorption caused by dry, dust-free air and scattering and absorption caused by atmospheric aerosols (Idso, 1969). These are considered in turn.

(a). Scattering by dry dust-free air.

If a volume  $dV$  of a scattering medium is irradiated from a direction defined by zenith angle  $\theta$  and azimuth angle  $\phi$  then for a solid angle element  $d\Omega = \cos \theta \sin \phi d\theta d\phi$  the radiant intensity  $I = d\Phi/d\Omega$  of the scattered radiation can be derived from:

$$(3). \quad d^2 I(\theta_i, \phi_i; \theta_s, \phi_s) = \gamma_{sc} \cdot L d\Omega dV$$

where the subscripts  $i$  and  $s$  refer to incident and scattered radiation respectively.  $\gamma_{sc}$  is the volume scattering function and from (3) is given by;

$$(4) \quad \gamma_{sc} = d^2 I / \int d\Omega dV$$

Integrating over all directional increments  $d\Omega$  defines the volume scattering coefficient which is a measure of the total radiation scattered from a single direction  $(\theta_i, \phi_i)$  to all directions;

$$(5). \quad \beta_{sc} = \int_{4\pi} \gamma_{sc} d\Omega$$

Instead of the scattering function  $\gamma$ , the scattering phase function is often used;

$$(6). \quad P = \frac{4\pi \gamma_{sc}}{\beta_{sc}}$$

This is basically the ratio of the radiance emitted in the direction ( $\psi$ ) to the mean radiance averaged over all directions (see fig.2)

If the wavelength of the radiation is greater than the characteristic length of scattering particles (as is the case in a dry dust-free atmosphere), the phase function for scattering angle  $\psi$  (the angle between incoming and outgoing rays) is given by;

$$(7). \quad P(\psi) = \frac{3}{4} (1 + \cos^2 \psi)$$

This type of distribution (see fig.2) is known as Rayleigh scattering (Platt and Partridge, 1975). The intensity of scattered radiation ( $I$ ) for scattering angle  $\psi$  is given by;

$$(8) \quad I(\psi, \lambda) = \alpha_R (\psi, \lambda) I(\lambda)$$

where  $\alpha_R$ , the volume scattering coefficient is calculated from the following relationship;

$$(9). \quad \alpha_R (\lambda) = \frac{8\pi^2}{3H\lambda^4} \cdot [n(\lambda) - 1]^2 \cdot P(\psi)$$

where  $H$  is the number of molecules per unit volume in the atmosphere,  $n(\lambda)$  is the refractive index of the molecules, and  $\lambda$  the wavelength of the incident flux.

In operational models of the earth's atmosphere simpler and more empirical relationships may be used. For example, a least square fit to the accurate values of Rayleigh scatter in a

'standard' atmosphere (Platt and Partridge, 1975) gives the following relationship;

$$(10) \quad \alpha_R(\theta) = 0.28 / (1 + 6.43 \cos \theta)$$

where  $\theta$  is the solar zenith angle.

(b) Absorption and scattering by aerosols.

The density distribution of air molecules with height in the atmosphere which gives rise to the Rayleigh scattering mechanism is relatively easy to quantify compared to the distribution of particles such as dust, smoke, cloud droplets etc. in the atmosphere. For situations where particle size is equal to, or greater than the wavelength of the incident radiation, analytical solutions of the attenuation problem are highly complex functions of particle size distributions, optical properties, density distribution etc. which are highly variable in time and space.

Scattering of radiation by aerosols (e.g. dust) is strongly forward peaked (see fig. 2) For this reason their contribution to the atmospheric albedo is often ignored and only Rayleigh scattering is accounted for (e.g. Platt and Partridge, 1975). Scattering of this type, however, does manifest itself quite strongly as a general deterioration of multispectral images (e.g. in atmospheric haze conditions).

In an homogenous absorbing medium equal fractions of the absorbing flux are absorbed over equal distances. Thus  $\Phi$  is reduced to  $\Phi - d\Phi$  in distance  $dz$ . Hence;

$$(11) \quad \frac{d\Phi}{\Phi} = -\mu dz$$

where  $\mu$  is coefficient of absorption of the medium (Slater, 1980).

In the atmosphere  $\mu$  is a complex function of density  $\rho$ , path length( $l$ ) and the type and distribution of the intervening aerosols. For the simplest case :

$$(12) \quad \frac{d\Phi}{\Phi} = -\mu(z) \rho(z) dz$$

where  $\mu$  is the coefficient of absorption of the medium (Slater, 1980).

Integrating (12) over path length ( $l$ ) yields :

$$(13) \quad \Phi(\lambda) = \Phi(\lambda_0) \exp \left[ \int_l \mu(z, \lambda) \rho(z) dz \right]$$

The integral is known as the optical depth and the exponential of this as the transmittance.

Analytical or numerical solutions (e.g using Monte Carlo simulation techniques) reflect the high complexity of attenuation by aerosols in the atmosphere. These are usually too cumbersome for use in operational models in remote sensing applications. Their main value is in providing a test bed for simpler parameterisations of atmospheric attenuation.

There exists a large number of more or less semi-empirical expressions for calculating the atmospheric attenuation of radiant flux. For clear skies equation (13) can be approximated by :

$$(14). \quad \bar{\Phi}(\lambda) = \bar{\Phi}(\lambda_0) \cdot \exp(-\tau_h \cdot m)$$

where  $\tau_h$  is the optical thickness of the atmosphere measured in the local zenith direction and  $m$  is the optical mass of the atmosphere which accounts for the increase in path length (1) with increasing zenith angle ( $m = \sec z$ ). Dave (1980) resolved the optical thickness ( $\tau_h$ ) of the atmosphere into four components ;

$$(15). \quad \tau_h = \tau_{R3} + \tau_{M3} + \tau_{am} + \tau_{o3}$$

where  $\tau_{R3}$  is the transmittance afforded by the Rayleigh scattering mechanism,  $\tau_{M3}$  is the transmittance afforded by the Mie scattering mechanism,  $\tau_{am}$  is the absorption moisture and  $\tau_{o3}$  is the absorption by ozone.

Values for each of these transmittances may found in standard sources such as the Smithsonian Meteorological Tables. Unfortunately , clear skies are relatively rare over Western Europe (for example, c.75% of all landsat images over Europe are obstructed by cloud, Eliason,1980).

The amount of cloud , its type and distribution often dominates tranfer of radiation to the ground. Many expressions make use of this factor. Elkington (1979) ,for example, used the following expression (after Gadd and Keers,1970).

$$(16). \quad E_s = S_0 (0.6 + 0.2 (\sin \beta)) \sin \beta \cdot C_R$$

PAGE 13

where  $E_s$  is the shortwave irradiance on the surface,  $S_0$  is the solar constant,  $\beta$  is the solar elevation and  $C_k$  is the cloud fraction.

(3.2) The reflectance properties of the earth's surface

There are five properties of reflected electromagnetic radiation which may be used to obtain information about the earth's surface subsequent to reflection. These are the phase, wavelength, intensity, direction of propagation and polarisation. Some measured properties, such as the intensity and the direction of propagation, are common to most remote sensing systems operating in the reflective wavelengths. Although the phase and polarisation have received less attention they may be in combination with the more widely used quantities such as wavelength.

The phase of an electromagnetic signal refers to the cyclical increment between one wave peak and another and is measured as an angle (e.g. between 0.0 and 2 radians.). It is only widely used in active systems using, for example lidars (Becker ,1980 ; Reeves 1975).

The combination of wavelength, intensity and direction of propagation of reflected radiation forms the instrumental basis of many remote sensing systems operating in the visible spectrum. Aerial photography using airborne cameras with film, or multispectral imaging scanners on satellite platforms (such as the Mercury 4, Gemini and Landsat satellites) are based on this combination. Hence, attention is given here to the physical principles underlying these systems.

A particular wavelength of electromagnetic energy arriving at the earth's surface is either reflected, absorbed or transmitted,(Goillot,1980) The proportions of energy

reflected, absorbed or transmitted will be dependent on the surface properties and upon the wavelength of the energy(Curran, 1980). This means that features similar at certain wavelengths in terms of their reflectivity are often clearly differentiated at other wavelengths (fig. 3) This provides the basis for differentiation o the earth's surface in terms of their "spectral signatures".(Price,1980). Slater (1980) defines the spectral signature of ground surface feature as a set of values for the reflectance or radiance of the feature rather than a fixed diagnostic value. The set of reflectance or radiance values obtained when an area is remotely sensed is peculiar to the irradiance , viewing geometry and the wavelength interval pertaining at that time. All these factors must be kept constant in order to seperate one area from another in terms of spectral reflectivity alone. Alternatively the spectral reflectivity of the surface as a function of irradiance, viewing geometry and wavelength interval must be determined.

The spectral reflectance of a surface relates the radiant exitance ( $M$ ) of that surface to its irradiance ( $E$ ). There are several reflectance measurements defined in the literature. Kimes (1980) discusses three expressions which are commonly used. These are the bi-hemispherical reflectance, the hemispherical-conical reflectance  $\rho_c$  and the bi-directional reflectance function ( $BDRF=\rho_B$ )

The bi-hemispherical reflectance  $\rho_H$  is defined as the ratio of the reflected exitance to the irradiance at the target surface.

$$(17.) \quad \rho_H = \frac{\int_0^{\pi} \int_0^{\pi/2} L_r(\theta_r, \phi_r) d\Omega_r}{\int_0^{\pi} \int_0^{\pi/2} L_i(\theta_i, \phi_i) d\Omega_i} = \frac{M}{E}$$

To establish the bi-hemispherical reflectance for a surface the irradiance and the radiant exitance integrated over all zenith and azimuth angles needs to be known. Although the total irradiance ( $E$ ) incident upon a surface may be calculated, remote sensing systems "sample" only a limited region of the reflected hemisphere. This region is defined by the viewing geometry and the instantaneous field of view of the radiometer.

If the reflecting surface is a perfect diffuser of incident radiation (i.e. it reflects radiation isotropically in all directions) then equation (17) reduces to;

$$(18). \quad \rho_h = \frac{\frac{E}{\pi} \int_0^{2\pi} \int_0^{\pi/2} d\Omega_r}{\int_0^{2\pi} \int_0^{\pi/2} L_i(\theta_i, \phi_i) d\Omega_i}$$

Surfaces which exhibit this type of behaviour are termed 'Lambertian'. In these cases, the region of the reflected flux sampled by the sensor is representative of the whole reflected hemisphere. This is rarely the case Kimes(1980) defines the hemispherical-conical reflectance factor  $\rho_c$  for a nadir looking sensor having a field of view of less than 2 steradians. It is the ratio of the reflected flux of a surface in the direction of the sensor's field of view (FOV) to the reflected flux of a perfectly reflecting horizontal Lambertian surface in the direction of the sensor's field of view.

$$(19). \quad \rho_c = \frac{\int_{\phi_i}^{\phi_a} \int_{\theta_i}^{\theta_a} L_r(\theta_r, \phi_r) d\Omega_r}{\frac{E}{\pi} \int_{\phi_i}^{\phi_a} \int_{\theta_i}^{\theta_a} d\Omega_i}$$

Although equations (18) to (19) assume anisotropic source radiance they fail to uniquely define the reflectance properties of the irradiated surface (which are assumed to be constant with time) since they are scalar quantities which deal only with the total irradiance and exitance of the surface rather than their directional characteristics. Thus for non-Lambertian surfaces both  $\rho_s$  and  $\rho_c$  will vary strongly as functions of viewing geometry and solar zenith angle. The bi-directional reflectance distribution function ( $\rho_b$ ) is a vector quantity and hence uniquely defines surface reflectance characteristics.

$$(20). \quad \rho_b(\theta_i, \phi_i; \theta_r, \phi_r) = \frac{dL_r(\theta_r, \phi_r)}{L_i(\theta_i, \phi_i) d\Omega_i}$$

Because of the difficulties involved in establishing for a natural surface, Lambertian, perfectly diffusing behaviour is often assumed in remote sensing applications. (Goillot, 1980). Only a few values of  $\rho_b$  have been derived for natural surfaces. Kriebel (1977) established some functions for flat vegetated surfaces (specifically savannah, bog, pasture land and coniferous forest). These functions are not valid, however, for inclined surfaces since the structure of vegetation in relation to incident changes with slope (Kimes and Kirchner, 1981). Because of these difficulties in using the bi-directional reflectance function many studies either assume that the target approximates to a Lambertian surface or alternatively the reflectance factors  $\rho_s$  or  $\rho_c$  as functions of solar zenith and azimuth angles and viewing geometry are established.

The lambertian assumption has been tested by several people under varying circumstances. It's inadequacies are clearly highlighted in areas of rugged or undulating topography where exitance values due to local reflectance of the surface may be difficult to seperate from anisotropic slope effects. Consequently most research has focused on establishing a spectrum of slope angles and azimuths over which the Lambertian assumption is valid for a given level of accuracy (Holben and Justice,1980; Smith et. al.,1980). Most of these studies, however, are limited to simple surfaces such as sand) and assume that the diffuse component of the incident radiation is negligible compared to the direct, specular component.

Although conceptually simple, the spectral reflectance of a non-Lambertian surface has been found to be very difficult to characterise in practice. Like most phenomena investigated by physical science, the reflective characteristics of the earth's surface can be looked at in two ways. It can be done by constructing more or less elaborate models based on the physics of the situation or alternatively by summarising a large amount of data in terms of a few empirical generalisations. The deterministic model developed by Suits (1972) is an example of the former whilst the derivation of a range of slope and illumination angles over the Lambertian assumption is valid is largely an empirical exercise. These are not mutually exclusive but rather form the extremes of a spectrum of possible approaches.

Several deterministic mathematical models have been developed to simulate the seasonal and diurnal reflectance trends of the earth's surface. Many of these are only applicable for a limited set of conditions. The model of Otterman (1981), for example, simulates the diurnal reflectance trends of a partially vegetated, desert surface. In this instance the nadir reflectance is dominated by the soil background. At low solar elevations, however, reflectance is controlled by the amount of shadow thrown by the clumps of vegetation. Kimes et. al.(1981) and Smith et. al.(1981) both describe complex energy balance models of fully developed canopies. In this model the reflectance of the canopy, which is divided into three horizontal layers, is calculated iteratively from the reflectance coefficients and the inclinations of the leaves within each layer. Several other models exist between these two extremes of partially and fully vegetated surfaces. All have varying degrees of complexity depending on how faithfully they try to represent the range of factors involved. These factors include variations in anisotropic sky irradiance, canopy geometry, the optical properties of the canopy components, the type of reflectance measurement, wavelength band, topography and instrumentation (Kimes et. al.,1980).

One of the most generalised treatments of surface reflectance is given in the model of Suits (1972). This is based on the Bouger law of transmission of electromagnetic energy through an absorbing medium (see equation .11). Thus:

$$(21). \quad \frac{d E_{ij}}{dz} = -\mu_{ij} E_{ij} + B_{ij}$$

where  $E_{ij}$  is the irradiance over layer  $j$  in the canopy for radiation component  $i$  (upward diffuse, downward diffuse and direct, specular components),  $\mu_{ij}$  is coefficient of absorption of layer  $j$ , component  $i$  and  $B_{ij}$  represents the addition or subtraction of radiant flux from one component to another (e.g. from specular to upward diffuse), (see fig.4).

For each layer ( $j$ ),  $\mu_{ij}$  is dependent on sun angle, leaf geometry and the optical properties of the component leaves. The leaf geometry is described for each layer in terms of the area projection of the individual leaves on a horizontal plane (the leaf area index) and on two orthogonal vertical planes (see fig. 5). If for the horizontal plane  $\sigma_h$  is defined as the average area of projection of the leaves and  $\eta_h$  is the number of horizontal projections per unit volume then the attenuation of diffuse flux through the horizontal plane is given by;

$$(22). \quad \mu_{ij} = \sigma_h \eta_h (1-\tau)$$

where  $\tau$  is the transmissivity of the individual leaves which may be derived from laboratory measurements. Analogous expressions are used for the area projections onto the vertical planes.

Although each leaf element within the canopy is assumed to be a Lambertian surface, the overall effect of the vertical components of the leaf geometry, described by the vertical area projections, is to produce anisotropic, nonLambertian reflectance characteristics. The model uses an iterative

procedure to calculate a 'self-consistent' radiant flow field (Suits, 1972). It assumes an isotropic flow field as a first approximation and progressively adjusts this until the radiance within the canopy is consistent with the reflected radiation from the detailed geometry of leaves and stems. For a more detailed description of the model see Suits(1972) or Slater(1980).

Figure 6. shows the variation of spectral reflectance with wavelength for a corn canopy at two different azimuth angles which was derived from the Suits model. It shows that the spectral reflectance, as well as its degree of change with viewing or illumination angle are both wavelength dependent. This factor must be taken into account when using broad band radiometers. For these instruments the value of  $\rho_H$  is also dependent on the range of wavelengths over which the reflected radiation is measured. Thus for broad band radiometers;

$$(23). \quad \rho_H = \frac{\int_{\lambda_1}^{\lambda_2} \rho_H(\lambda) \cdot F(\lambda) \cdot R(\lambda) d\lambda}{\int_{\lambda_1}^{\lambda_2} F(\lambda) \cdot R(\lambda) d\lambda}$$

where  $R(\lambda)$  is the spectral responsivity of the detector. This factor, when not accounted for, may produce diurnal reflectance trends as measured by broad band radiometers which are merely artifacts of the measurement procedure (Kimes et al., 1980).

Changes in spectral reflectance which are indicative of change in canopy structure are of interest to a variety of disciplines. The seasonal reflectance trend may, for example, be used to predict the yield from a wheat harvest, (Hatfield

et. al. 1975), whilst moisture stress is manifested as a decrease in reflectance of the infra-red band(0.7um to 1.3um) by vegetation. A multispectral image of moisture stressed vegetation will thus show a characteristic increase in the blue-green response of the canopy at the expense of the infra-red response. This factor has been used by Wehemannen and Thompson (1979), who devised a Green Index Number (GIN) to be used with Landsat data. This statistic correlates well with moisture stress in the wheat-growing regions of the Great Plains of the U.S.A. and eastern Australia. The high infra-red reflectance of healthy vegetation can also be reduced by several other factors however. In practice it is often difficult to distinguish between changes in reflectance brought about by disease and by moisture stress.

For exposed soil surfaces, more direct information concerning the moisture content of the soil can be gained through the use of reflectance data (Idso et. al.,1975). In general bare soils of varying types have an increasing reflectance with wavelength and a decreasing reflectance with moisture content (Hardy, 1980),(see figure 7). Many other factors, however, interact to give a particular soil surface its reflective characteristics. A decrease in grain size, for example, will produce an increase in reflectance due to the reduction in the area of shadow, the smoother surface and hence the decrease in overall extinction of incident flux. Fine textured soils are, however, usually darker than coarse textured soils on aerial photographs due to their greater moisture retention properties (Reeves, 1975). Other

complicating factors include the presence of a surface veneer of strongly coloured minerals (e.g. iron oxides), humus staining, surface roughness and illumination angle. Furthermore reflectance values are only characteristic of a narrow layer of soil (c. 1-2cm.), (Idso et. al., 1975). A soil which is saturated at a depth of 3cm. but is dry in its uppermost layer due to a high evaporative demand will therefore have its bulk properties misrepresented by reflectance data. Thus the determination of soil moisture alone from reflectance data (except in relative cases) requires a large amount of auxiliary data about the character of the soil itself.

Finally the polarisation of surface reflected light may be used as an indicator of soil moisture content (Curran, 1978). Light reflected from natural surfaces is diffuse whereas that reflected from water is strongly specular (see (fig.8)). In general, the more specular the reflection, the greater the degree of polarisation imparted at reflection. Consequently near-Lambertian surfaces do not impart much polarisation (Slater, 1980). Diffuse reflection of light is caused by multiple reflections within the depth of soil it penetrates. The finer or less structured a soil, the smoother the surface it presents to incident radiation. The same role is played by moisture which restricts space for multiple reflection between particles and hence restricts Lambertian behaviour.

The relationship between the polarisation of light reflected from soils and their soil moisture content is shown in fig 8. the best correlation occurs within the mid-range of moisture values, rather than at the extremes , (i.e., saturated and dry soils) (Curran, 1979).

Like reflectance data in general, the use of polarised light in the remote sensing of soil moisture is restricted by the number of variables affecting it. Roughness and texture variations tend to mask variations in soil moisture whilst a vegetation cover adds its own diffuse component to the reflected light. Again depth penetration is limited to 1-2cm.

(4). Data processing systems in remote sensing.

For any scene viewed by a radiometer from an airborne or satellite platform, the resultant image is a function of the relationships between the incident radiation and the vegetation cover (leaf physiology and geometry etc.) the soil background(texture, mineralogy, moisture), solar angle, the viewing geometry (orbital characteristics, topography etc.) and the prevailing meteorological conditions. The information content of a single image is therefore potentially very large. Because of this high information content, together with voluminous amount of data that can be produced by a single system (Landsat, for example produces 10 bits per year, Verhagen et. al., 1980) processing systems are highly automated and computerised.

Numerous specialists (geographers, geologists, ecologists etc.) are actively engaged in image interpretation. All have varying requirements. Geologists and soil scientists may be interested in the reflectance from bare soil or rock without the interference of vegetation, whilst agricultural specialists may wish to view vegetation at its most vigorous stage of growth. Thus conflicts inevitably occur in relation to timing of overpass, scale and resolution of image etc. (Allan, 1980). The use of selective processing techniques allows a more flexible use to be made of the data available.

The techniques commonly used to extract relevant information from remotely sensed data come under the broad heading of "pattern recognition" (Verhagen et. al., 1980). Pattern recognition involves the identification of pattern (structure, order etc.) within a complex set of data (Swain, 1978). A pattern recognition system is represented graphically in figure 10. Most systems have three component stages.

1) The Sensor;

This may measure any portion of the electromagnetic spectrum, microwave, visible reflective, thermal infra-red, gamma ray etc. A knowledge of the characteristics of the sensor, its orbital parameters, the band sensitivities of the radiometer etc. , is vital for an interpretation of the remotely sensed data. The Landsat 3 MSS system, for example, produces a continuous strip image of the earth's surface, 185

km. wide at four wavelength bands. These are referred to as bands 4 (blue-green), 5 (orange-red) and 6 and 7 (infra-red). Each Landsat image is made up of picture elements (pixels) representing a ground area of 79 m. by 79 m. Due to overlapping between each separate swath path the effective spatial resolution of an image is 70 m. along track, and 57 m. cross track. Each pixel is recorded at one of 64 possible brightness values (Slaney, 1981). The Landsat series has considerably increased the already large quantity of data available in the visible and reflective infra-red portions of the spectrum. This stems from the earlier development of aerial photography. Data and imagery from space platforms has been available since the early 1960's (Mercury 4 and Gemini satellites).

2) The Preprocessor;

This stage involves the transformation and reduction of data in order to find attributes or features relevant to the investigation. This may involve the reduction of random noise effects (caused by atmospheric scattering and radiometer defects) through filtering or the wholesale transformation of input data to eliminate systematic errors (e.g. caused by the earth's spin and curvature) or the selective transformation of the data to produce desired effects. A wide array of techniques are available for selective use of the data. These include band ratioing, edge enhancement, cluster analysis etc. Some of the more popular band ratioing algorithms, together

with their uses are listed in Table 1. Multispectral scanner data can often be correlated (e.g. through principal components analysis) to reduce the amount of data giving uncorrelated features (Morrison and Scherer, 1977).

3) The Classifier;

This may be a trained human investigator confronted with the transformed data in easily digestible and interpretable form. Alternatively an automated classification procedure may be used such as a clustering algorithm. The classification procedure may be supervised or unsupervised. The former depends on a set of 'training data' collected in the field independently of the remotely sensed data which is then used to establish the criteria for the classification. Unsupervised procedures, on the other hand, are entirely based on regularities within the data itself.

The information extracted by these techniques has value in many areas of research (geological, agricultural, geographical etc.). Practical applications include operational yield estimates using Landsat MSS data as one of the inputs. The Large Area Crop Inventory Experiment (LACIE), for example, uses data on hydrology, climate, terrain, and MSS reflectance data to predict yield and area of production in wheat growing areas of America (Erb, 1980).

(5). General Discussion

Remote sensing from airborne and space platforms has several important advantages over alternative means of resource evaluation which are based on interpolation between point samples. The ability of remote sensing systems to make quick and frequent inventories of earth resources over large areas is their most attractive feature. These inventories fall into two categories (Hardy, 1980).

(a). The surveying of relatively static earth surface features such as lithology, soil type and topography.

(b). The survey and subsequent monitoring of more dynamic phenomena such as weather systems, soil moisture or vegetation.

Many properties of the earth's surface (such as vegetative cover) may be arbitrarily placed in either category. Soil moisture content, however, is firmly embedded in the latter group of highly dynamic phenomena. Although an initial survey may be able to determine how much moisture a soil can hold between field capacity and wilting point, its soil moisture status at any point in time can only be ascertained through frequent monitoring.

The decision to use remotely sensed data an alternative to regional estimates of soil moisture from precipitation and potential evaporation data is an economic one (Hardy, 1980). However, the more technological problem of devising a remote

sensing system that works has still to be solved As yet there is no fully operational method for calculating soil moisture over a large area from remotely sensed data although there are several candidates. With this in mind the physical principles of remote sensing in the visible and reflective waveband have been reviewed above.

There exists a large quantity of data in the visible and reflective infra-red portions of the electromagnetic spectrum. The continuation of the Landsat series (Landsat D is to be launched in 1982) together with the launch of European satellites such as SPOT (due to be launched in 1984, Smith, 1981) means that an even larger reservoir of data will be available for research purposes. Because of the ready availability of this data, its potential for the remote sensing of soil moisture must be fully explored. In practice, however, reflectance data collected in this region of the spectrum has some major limitations for the remote sensing of soil moisture. To obtain a reliable and quantitative estimate of soil moisture content, the effects of vegetation, surface roughness, topography, mineralogy and meteorological conditions have to be known. Furthermore the limited depth resolution of reflectance data(c.2cm.) means that it is often poorly correlated with bulk soil properties such as soil moisture. If, however, suitable ground data is available to supplement the reflectance data, routine measurement may be possible, especially if only relative values of soil moisture content are required. Reflectance data alone, without any auxiliary ground and meterological data remains ambiguous in interpretation.

REFERENCES

- Curran P.J.  
1979  
The Use of Polarized Panchromatic and False Colour Infrared Film in the Monitoring of Soil Surface Moisture  
Remote Sensing of Environment Vol 8:249-266
- Curran P.J.  
1978  
A Photographic Method for the Recording of Polarized Visible Light for Soil Surface Moisture Indications  
Remote Sensing of Environment Vol. 7 pp 305-322
- Dozier J. Frew J.  
1981  
Atmospheric Corrections to Satellite Radiometric Data over Rugged Terrain.  
Remote Sensing of the Environment Vol. 11 pgs 191-205
- Dozier J. Outcalt S.I.  
1979  
An approach toward Energy Balance Simulation over Rugged Terrain  
Geographical Analysis Vol. 11 no.1
- Dozier J.  
1980  
A Clear Sky Spectral Solar Radiation Model for Snow Covered Mountainous Terrain.  
Water Resources Research Vol. 16 no. 4 pgs 709-718
- Eliason P.T. Soderblom L.A. Chavez P.S.  
1981  
Extraction of Topographic and Spectral Albedo Information from Multispectral Images.  
Photogrammetric Engineering and Remote Sensing Vol.48 no.11 pp 1571-1579
- Elkington M.D.  
1979  
An approach to characterising the water content of soils by thermalinfrared remote sensing  
Working Paper no.262.
- Erb R.B.  
1980  
The Large Area Crop Inventory Experiment (LACIE).  
Chapter 19 in "Remote Sensing Application in Agriculture and Hydrology. (edited by G. Fraysse)
- Gadd A.J. Keers J.F.  
1970  
Surface Exchanges of Sensible and Latent Heat in a 10-Level Model Atmosphere  
Quarterly Journal of the Royal Meteorological Society Vol. 96 pp. 297-308
- Gieger R.  
1966  
The Climate near the Ground  
Harvard University Press , Cambridge , Massachusetts.
- Gillespie A.R. Kahle A.B.  
1977  
Construction and Interpretation of a Digital Thermal Inertia Image

Photogrammetric Engineering and Remote Sensing Vol.43 no.8 pp 983-1000

Goillot Ch. C.  
1980

Significance of Spectral Reflectance for Natural Surfaces  
in Remote Sensing Applications in Agriculture and Hydrology ; Chapter 6 (edited  
by G. Fraysse)

Green F.H.W. Harding R.J.  
1979

The Effects of Altitude on Soil Temperature  
Meteorological Magazine Vol. 108 pgs 81-91

Harding R.J.  
1979  
Radiation in the British Uplands.  
Journal of Applied Ecology Vol. 16 pgs 161-170.

Hardy J.R.  
1980  
Survey of Methods for the Determination of Soil Moisture Content by Remote  
Sensing Methods.  
Chapter 14. in "Remote Sensing Application in Agriculture and Hydrology.

Hatfield J.L. Reginato R.J. Jackson R.D. Idso S.B. Pinter P.J.  
1978  
Remote Sensing of Surface Temperature for Soil Moisture, Evapotranspiration and  
Yield Estimation.  
Fifth Canadian Symposium on Remote Sensing , Victoria. pp 460-466

Holben B.N. Justice C.O.  
1980  
Topographic Effect on the Spectral Response from Nadir-Pointing Sensors.  
Photogrammetric Engineering and Remote Sensing Vol.46 pp 1191-1200.

Holben B.N. Justice C.O.  
1980  
The Topographic Effect on Spectral Response from Nadir-Pointing Sensors  
Photogrammetric Engineering and Remote Sensing Vol.46 pp. 1191-1200

Idso S.B. Jackson R.J. Reginato R.J. Kendall B.A. Nakayama F.S.  
1975  
The Dependence of Bare Soil Albedo on Soil Water Content  
Journal of Applied Meteorology Vol.14 pgs 109-113

Idso S.B. Reginato R.J. Jackson R.D.  
1974  
The Three Stages of a Drying of a Field Soil  
Soil Science Society of America (Proceedings) Vol. 38 pp 831-837

Kimes D.S Smith J.A. Link L.E.  
1981  
A Thermal IR Exitance Model of a Plant Canopy  
Applied Optics Vol.20 no.4 pp. 623-632

Kimes S.K. Kirchner J.A.  
1981  
Modeling the Effects of Various Radiant Transfers in Mountainous Terrain on

Sensor Response.  
IEEE Transactions on Geoscience and Remote Sensing Vol. GE-19 no. 2 pp 100-108

Kriebel K.T.  
1978

Average Variability of the Radiation Reflected by Vegetated Surfaces due to  
Differing Irradiations.  
Remote Sensing of Environment Vol. 7 pp 81-83

Otterman J.

1981

Remote Sensing of a Complex Surface  
in "Remote Sensing in Meteorology, Oceanography and Hydrology" edited by A.P  
Cracknell; John Wiley and Sons, New York. pp 198-204.

Paltridge G.W. Platt C.M.R.  
1976

Radiative Processes in Meteorology and Climatology - Developments in  
Atmospheric Science 5  
Elsevier Scientific Publishing Company , Oxford.

Reeves R.G.  
1975

Manual of Remote Sensing ; Vol.1 Theory , Instruments and Techniques Vol.2 :  
Interpretation and Applications  
American Society of Photogrammetry, Falls Church, Virginia.

Slater P.N.  
1980

Remote Sensing; Optics and Optical Systems  
Addison-Wesley, Massachusetts.

Smith J.A. Lin T.L. Ranson K.J.  
1980

The Lambertian Assumption and Landsat Data  
Photogrammetric Engineering and Remote Sensing Vol. 46 no. 9 pp. 1183-1189.

Suits G.H.  
1972

The Calculation of the Directional Reflectance of a Vegetative Canopy  
Remote Sensing of Environment Vol. 2 pp.117-125

Swain P.H. Davis S.M.  
1978

Remote Sensing : The Quantitative Approach  
McGraw-Hill , New York.

Thompson D.R. Wehemann O.A.  
1979

Using Landsat Digital Data to Detect Moisture Stress  
Photogrammetric Engineering and Remote Sensing Vol. 45 no. 2 pp 201-207

Van Bavel C.H.M. Hillel D.I.  
1976

Calculating Potential and Actual Evapotranspiration from a Bare Soil Surface  
by Simulation of Concurrent Flow of Water and Heat  
Agricultural Meteorology Vol. 17 pp 453-476

Verhagen C.J.D.M. Duin R.P.W. Groen F.C.A. Joosten J.C. VerBeek P.W.  
1980  
Progress Report on Pattern Recognition  
Reports on Progress in Physics Vol. 43 pp 785-833

ACKNOWLEDGEMENT

The author is grateful to his Supervisor Dr J. Hogg for his help, advice and encouragement throughout the time of his research.

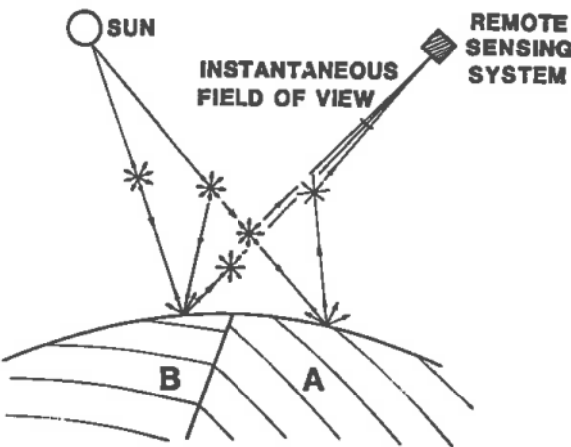


**FIG. 1. SCATTERING AND ATTENUATION OF INCIDENT AND REFLECTED FLUX BY THE ATMOSPHERE**  
(AFTER SLATER, 1980)

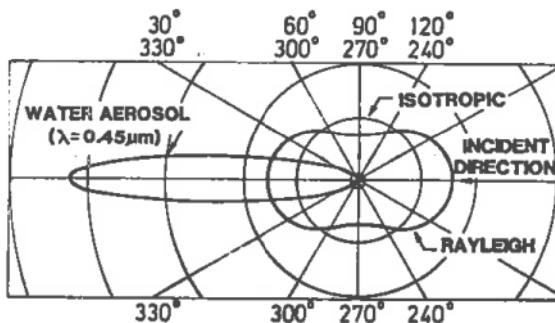


**FIG. 2. ANGULAR DEPENDENCE OF SINGLE-SCATTERING PHASE FUNCTIONS IN ANY AZIMUTHAL PLANE.**  
THE ISOTROPIC AND RAYLEIGH FUNCTIONS HAVE BEEN MULTIPLIED BY 10.  
(AFTER LA ROCCA AND TURNER, 1975. REPRODUCED FROM SLATER 1980)

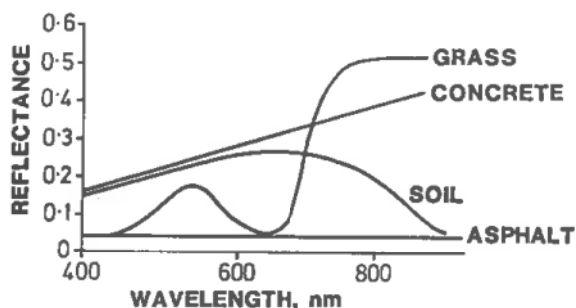


**FIG. 3. TYPICAL SPECTRAL REFLECTANCE CURVES FOR GRASS, CONCRETE, SOIL AND ASPHALT**  
(AFTER SLATER, 1980)

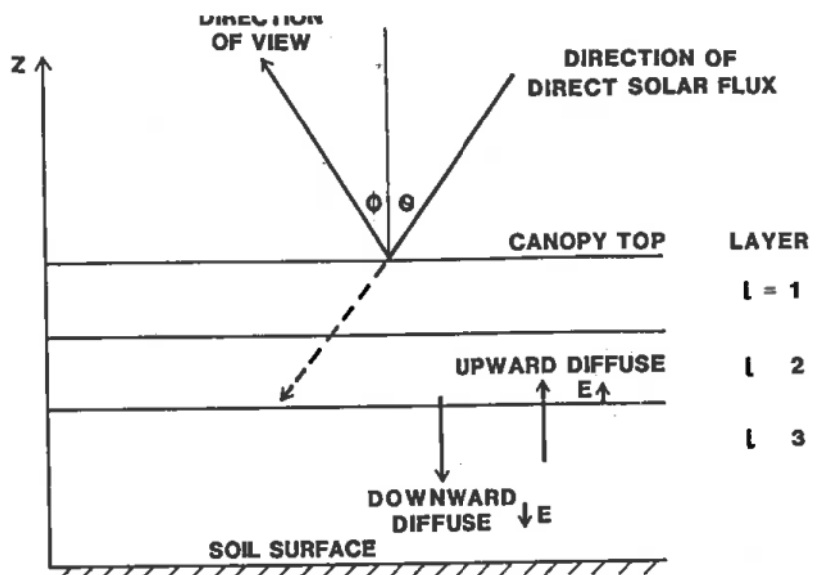


**FIG. 4. LAYERED CANOPY MODEL USED IN THE REFLECTANCE  
MODEL OF SUITS (1972). (AFTER SLATER 1980)**

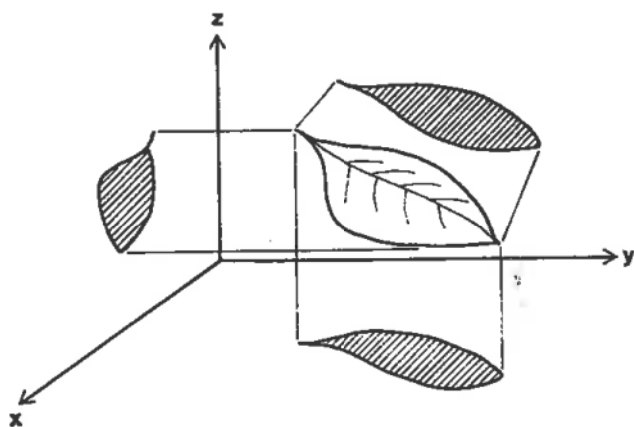


**FIG. 5. AREA PROJECTIONS OF LEAF ONTO 3 ORTHOGONAL  
PLANES (AFTER SUITS, 1972)**

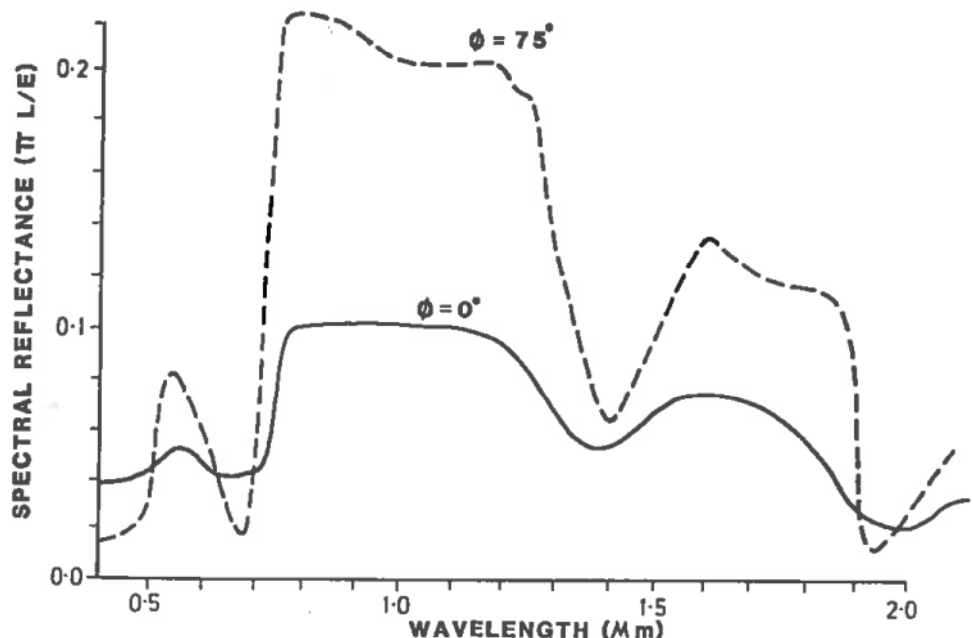


FIG. 6. DIRECTIONAL REFLECTANCE OF A CORN CANOPY. THE SPECTRAL REFLECTANCE CHANGES WITH VIEW ANGLE ( $\phi$ )

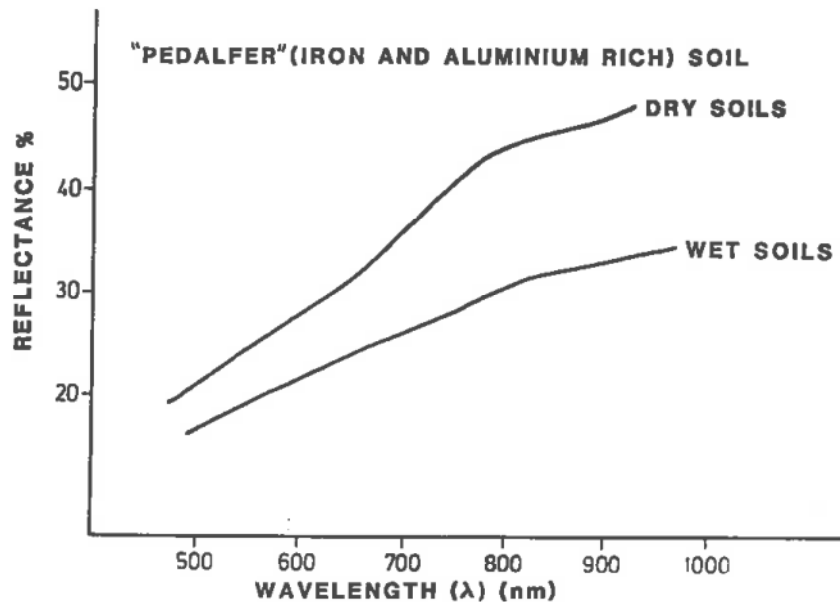
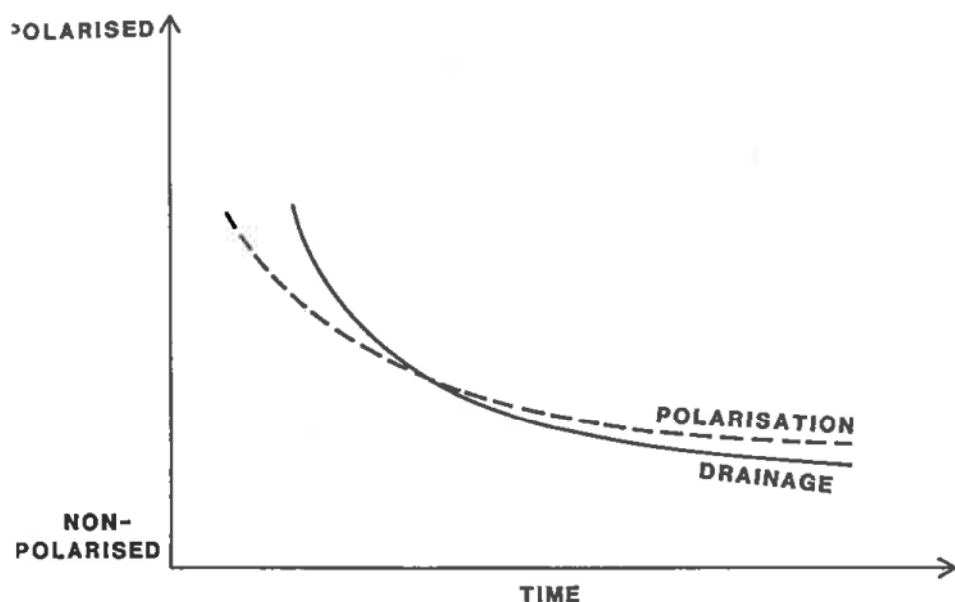
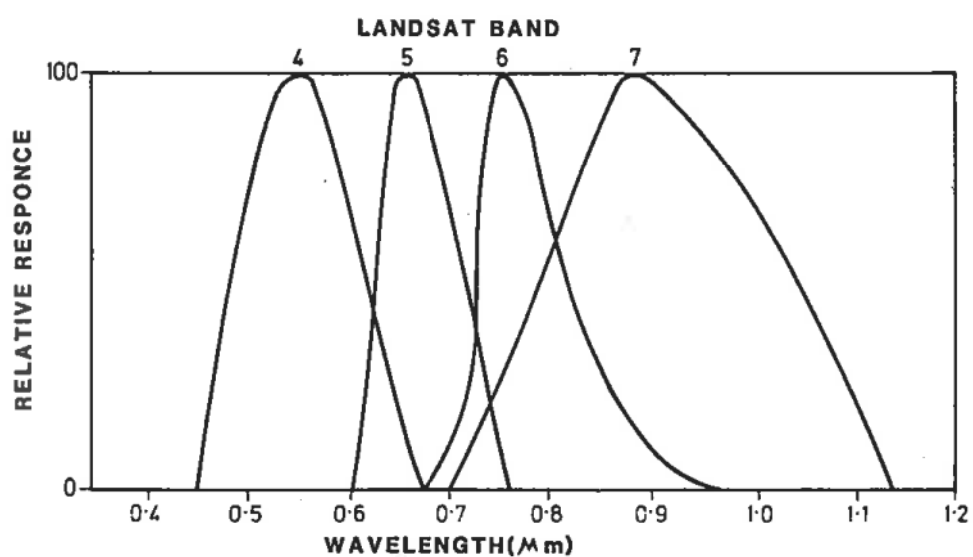


FIG. 7. THE RELATIONSHIP BETWEEN REFLECTANCE, SOIL MOISTURE AND WAVELENGTH IN THE VISIBLE BAND. (AFTER HARDY, 1980)



**FIG. 8. CORRELATION BETWEEN POLARISATION OF LIGHT AND STAGE IN DRAINAGE (DRYING) CURVE FOR SOIL (AFTER CURRAN, 1978)**



**FIG. 9. THE SPECTRAL RESPONCE OF THE MILTON MULTI-BAND RADIOMETER IN THE FOUR LANDSAT BANDS (AFTER CURRAN, 1980)**

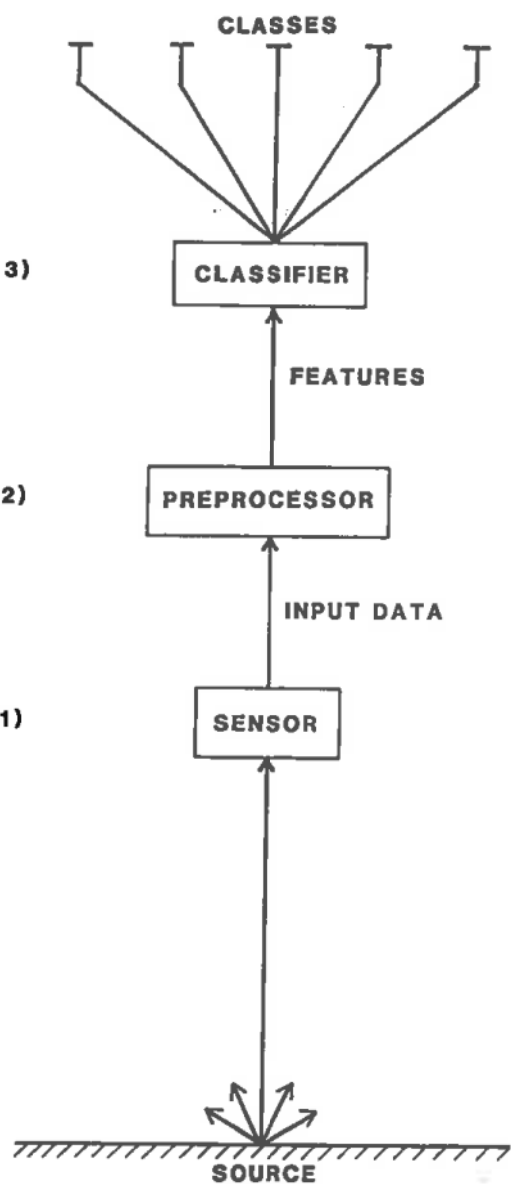


FIG. 10. A PATTERN RECOGNITION SYSTEM





Produced by  
School of Geography  
University of Leeds  
Leeds LS2 9JT  
From whom copies may be obtained